



Assessment of the Weather Research and Forecasting (WRF) Model for Extreme Rainfall Event Simulations in the Upper Ganga Basin

Ila Chawla^{1,5}, Krishna K Osuri^{3,4}, P P Mujumdar^{1,2} and Dev Niyogi^{4,5}

5 ¹Department of Civil Engineering, Indian Institute of Science, Bangalore, 560012, India

²Divecha Centre for Climate Change, Indian Institute of Science, Bangalore, 560012, India

³Department of Earth and Atmospheric Sciences, NIT Rourkela, Odisha, 769008, India

⁴Department of Agronomy- Crops, Soils, Water Sciences, Purdue University, West Lafayette, IN 47907, USA

⁵Department of Earth, Atmospheric and Planetary Sciences, Purdue University, West Lafayette, IN 47907, USA

10 *Correspondence to:* P P Mujumdar (pradeep@civil.iisc.ernet.in)

Abstract. Reliable estimates of extreme rainfall events are necessary for an accurate prediction of floods. Most of the global rainfall products are available at a coarse resolution, rendering them less desirable for extreme rainfall analysis. Therefore, regional mesoscale models such as the Advanced Research version of the Weather Research and Forecasting (WRF-ARW) model, are often used to provide rainfall estimates at fine grid spacing. Modelling heavy rainfall events is an enduring challenge, as such events depend on multiscale interactions, and the model configurations such as grid spacing, physical parameterization and initialization. With this background, the WRF-ARW model is implemented in this study to investigate the impact of different processes on extreme rainfall simulation, by considering a representative event that occurred during 15 – 18 June 2013 over the Ganges basin in India, which is located at the foothills of the Himalayas. This event is simulated with ensembles involving four different microphysics (MP), two cumulus (CU) parameterizations, two planetary boundary layer (PBL), and two land surface physics options; and different resolutions (grid spacing) within the WRF model. The simulated rainfall is evaluated against the observations from 18 rain gauges and the Tropical Rainfall Measuring Mission Multi-Satellite Precipitation Analysis (TMPA) 3B42RT version 7 data. From the analysis, it is noted that the selection of MP scheme influences the spatial pattern of rainfall, while the choice of PBL and CU parameterizations influence the magnitude of rainfall in the model simulations. Further, WRF run with Goddard MP, Mellor–Yamada–Janjic PBL and Betts–Miller–Janjic’ CU scheme is found to perform ‘best’ in simulating this heavy rain event. The model performance improved through incorporation of detailed land surface processes involving prognostic soil moisture evolution in Noah scheme as compared to the simple Slab model. To analyze the effect of model grid spacing, two sets of downscaling ratios – (i) 1:3, Global to Regional (G2R) scale; and (ii) 1:9, Global to Convection-permitting scale (G2C) are employed. Results indicate that higher downscaling ratio (G2C) causes higher variability and consequently, large errors in the simulations. Therefore, G2R is opted as a suitable choice for simulating heavy rainfall event in the present case study. Further, the WRF simulated rainfall is found to exhibit least bias when compared with that of the Coordinated Regional Climate Downscaling Experiment (CORDEX) data and the NCEP FiNaL (FNL) reanalysis data.

35 **1. Introduction**

Indian Summer Monsoon Rainfall (ISMR) is often associated with very heavy (124.5 to 244.4 mm/day) to extremely heavy (more than 244.5 mm/day) rainfall (Ray et al., 2014), particularly during June to September (Srinivas et al., 2013). The extremely heavy rainfall events often occur due to the presence of organized meso-convective systems (MCSs) embedded in large scale monsoonal features such as offshore troughs and vortices, depressions over the Bay of Bengal /Arabian Sea, and mid tropospheric cyclones (Sikka and Gadgil, 1980; Benson Jr and Rao, 1987; Zipser et al., 2006).

Extremely heavy rainfall at shorter time scales are particularly difficult to predict in mountainous terrains, and continue to be a challenge to operational and research community (Das et al., 2008; Li et al., 2017). Because of the multiscale features associated with these events, there has been an ongoing effort to implement mesoscale Numerical Weather Prediction (NWP) models for the ISMR simulations. The operational and research community has widely adopted the Advanced Research version of the Weather Research and Forecasting (WRF-ARW) model (hereafter referred as the WRF model), to simulate a variety of high impact meteorological events, such as rainfall (Vaidya and Kulkarni, 2007; Deb et al., 2008; Kumar et al., 2008; Chang et al., 2009; Routray et al., 2010; Mohanty et al., 2012), tropical cyclones (Raju et al., 2011; Routray et al., 2016; Osuri et al., 2017b) and thunderstorms (Madala et al., 2014; Osuri et al., 2017a). However, setting up the WRF model, that simulates extremely heavy rainfall over the ISMR region is still considered as a challenging task, which involves consideration of several aspects such as forcing data, model grid spacing/resolution, land surface parameterization and choice of an appropriate physics scheme.

Earlier studies such as by Krishnamurthy et al., (2009); Misenis and Zhang (2010); Rauscher et al., (2010); Mohanty et al., (2012); Chevuturi et al., (2015) indicated that heavy rainfall predictions can be improved through ensemble model techniques and fine grid resolution. However, the influence of the model parameterization schemes on mesoscale rainfall simulations over India is still an understudied issue. In particular, heavy rain simulations studies have reviewed the impact of individual parameterization options such as the Microphysics (MP) scheme (Rajeevan et al., 2010; Raju et al., 2011; Kumar et al., 2012), Cumulus (CU) parameterization scheme (Deb et al., 2008; Mukhopadhyay et al., 2010; Srinivas et al., 2013; Madala et al., 2014), Planetary Boundary Layer (PBL) scheme (Li and Pu, 2008; Hu et al., 2010; Hariprasad et al., 2014), and Land Surface Model (LSMs) options (Chang et al., 2009). However, the ensemble analysis that reviews the relative impact of different configurations is lacking. It is important to study the impact of different parameterizations in an ensemble mode because it is often likely that the performance of one scheme depends on other model configurations considered. For example, the conclusions regarding which CU scheme performs best would be intimately tied to the choice of the MP or land surface options considered in conducting the numerical experiments. With this perspective, an attempt is made in this paper, to assess sensitivity of the WRF model to predict an extremely heavy rainfall episode, that occurred from 15 June through 18 June 2013, over the Ganges basin in India, which is located at the foothills of the Himalayas. Additional details regarding the event are presented ahead. The performance of the WRF model is evaluated against the global reanalysis and downscaled data.



Thus, the tasks undertaken in this work are: (i) quantitative verification of the WRF model to simulate an extremely heavy rainfall event; (ii) assessment of sensitivity of the model simulated rainfall to different parameterization options, downscaling ratios and land surface models; and (iii) comparison of the WRF simulated rainfall with the global reanalysis data and the Coordinated Regional Climate Downscaling Experiment (CORDEX) downscaled data to investigate the impact of local versus global factors on rainfall simulations. A related objective is to use the model results and provide recommendations on a possible optimal choice for model configuration to simulate such events in the region.

Description of the heavy rainfall event

The 2013 summer monsoon had a normal onset but the trough advanced rapidly, covering whole of India by mid-June, instead of mid-July (Ray et al., 2014). This large-scale setting is thought to have created a platform for interaction of two synoptic scale events – northwest moving depression from Bay of Bengal and preexisting westerly trough in mid-troposphere. Meteorological studies conducted over the region (Kotal et al., 2014; Ray et al., 2014; Rajesh et al., 2016) established that there was a monsoon low pressure system during this period. The longitudinal time section for 850 hPa geopotential height along with anomaly averaged over 20° – 26° N showed high negative anomaly on 14 June, which migrated to west, over 75° E by 17 June. The meridional wind anomaly within the belt of 35° – 45° N showed a westerly wave, moving from 10° E on 12 June to 70° E on 17 June. These two anomalies are found to be in phase, consequently causing interaction between the eastward moving trough in mid-upper troposphere and westward moving monsoon low in the lower troposphere. The monsoon low provided the moisture feed and the upper level westerly trough provided the divergence to lift the moisture. This whole system eventually led to an unanticipated heavy rainfall during 15 – 18 June 2013 in the Kedarnath valley and adjoining areas in the state of Uttarakhand, India (Kotal et al., 2014; Ray et al., 2014; Rajesh et al., 2016). The region received rainfall greater than 370 mm in one day (17 – 18 June 2013), which is 375% above the daily normal rainfall (65.9 mm) during the monsoon season (Ray et al., 2014). Consequently, heavy floods occurred in the region, causing unprecedented damage to life and property.

The synthesis of the synoptic setting of the event has been carried out in a number of studies (Dube et al., 2014; Kotal et al., 2014; Ray et al., 2014; Shekhar et al., 2015; Rajesh et al., 2016), but the mesoscale assessment pertaining to the simulation of this rainfall event is still lacking. Therefore, the present study emphasizes on quantitatively evaluating and conducting sensitivity analysis on the prediction capability of the WRF model on rainfall simulations.

Since the epicenter of the heavy rainfall was Kedarnath, study region comprising of the upstream part of the Ganga Basin in India, referred as Upper Ganga Basin (UGB) hereafter, is selected in this paper. Figure 1 presents the topography of the UGB as described for the three Domains of the WRF (Domain 1, Domain 2a and Domain 2b with 27, 9 and 3 km grid resolution respectively) along with the 18 rain gauge stations located within the region. The region is of social, cultural and economic importance to India, further making this study necessary.

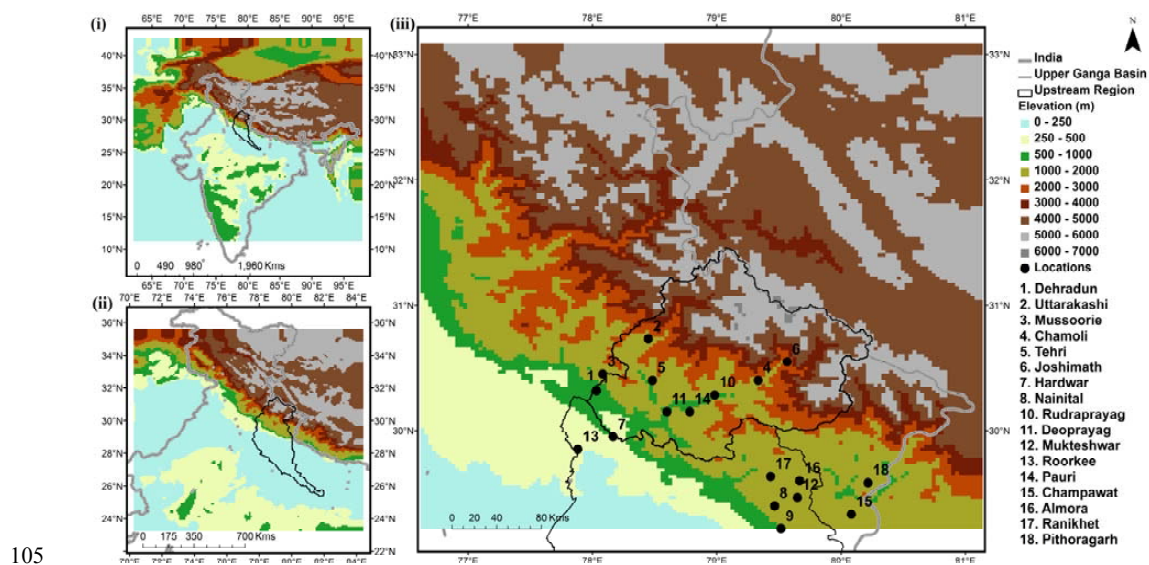
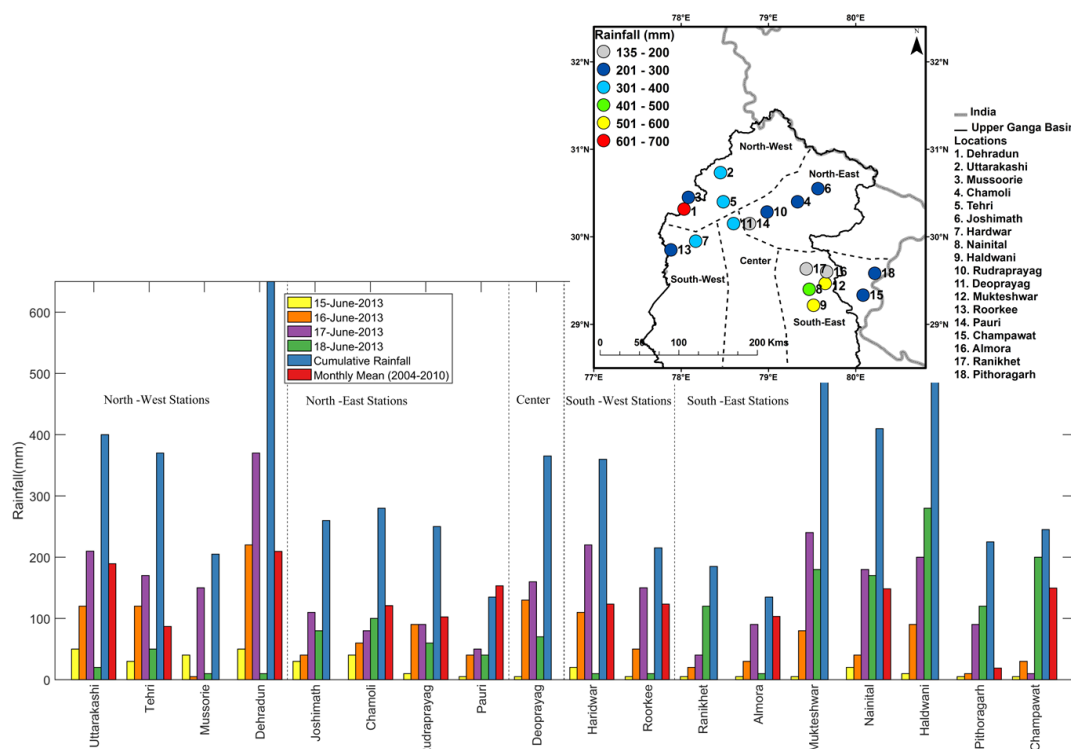


Figure 1. Topography of the study region (shown with black outline) as represented in the WRF model for (i) Domain 1 – 27 km grid spacing; (ii) Domain 2a – 9 km grid spacing (downscaling ratio – 1:3); and (iii) Domain 2b – 3 km grid spacing (downscaling ratio – 1:9). Locations of the rain gauge stations within the UGB are presented as black dots in Figure 1 (iii).

2. Data and Experimental Setup

110 2.1 Observed Data

Figure 2 presents daily and cumulative rainfall data from 15 to 18 June 2013 (obtained from the Indian Meteorological department (IMD) and literature (Ray et al., 2014) for the 18 official rain gauges located within the UGB.



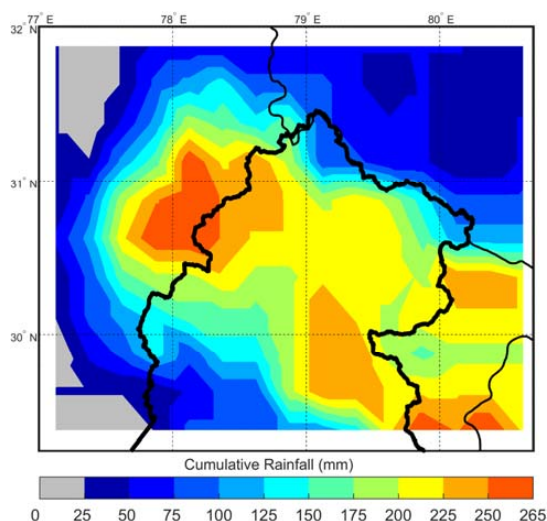
115 **Figure 2.** Observed daily and cumulative rainfall along with historic monthly mean (2004 – 2010) values at the 18 rain gauges in the upstream region of the UGB.

It is noticed that the northwest part of the region received higher rainfall compared to the northeast, with stations such as Tehri and Dehradun showing 327% and 210% (respectively) more rainfall than their historic means. A few stations like Chamoli in the northeast region, received 250 mm of cumulative rainfall over the 4 days' period, which is 144% higher than the historic mean. In general, most of the stations in the southern part of the basin, which are located at lower elevation, recorded relatively less rainfall with a cumulative range of 445 mm, in comparison to the northern part (at higher altitude) having a rainfall range of 515 mm. Additionally, three stations in the southeast region, i.e., Mukteshwar, Haldwani and Nainital received extremely heavy rainfall with a cumulative average of 498 mm. From the above analysis, it is evident that the system moved from east to west direction with two distinct regions in the UGB – southeast and northwest, receiving extremely heavy rainfall.

The region has complex topography and a limited number of rain gauges because of the difficulty in operating a network in this region. To further capture the spatial variability in rainfall, Tropical Rainfall Measuring Mission Multi-Satellite Precipitation Analysis (TMPA) 3B42RT (version 7) product, which is available at 0.25° resolution at daily scale is analyzed (Fig. 3). It is to be noted that, since the focus area for the analyses is the upstream region of the UGB (Fig. 1 (iii) and Fig. 2), results are presented in this paper with respect to the geographical extent of Domain 2b throughout this paper. From Figure 3, it can be noted that the TMPA data is able to capture the spatial variability in the rainfall – with distinct clusters corresponding to heavy rainfall in the northwest and southeast



regions of the study area. However, the rainfall amount is significantly underestimated by the TMPA product, with the maximum value of 265 mm against the recorded 650 mm. This under reporting for gridded satellite product
 135 versus rain gauge in the ISMR region is a well-known feature (Rahman et al., 2009; Kneis et al., 2014). The TMPA estimates are verified against the IMD station observations for baseline quality check. Mean absolute error (*MAE*), root mean square error (*RMSE*) and bias (β) are computed using the nearest neighborhood mapping approach and are presented in Table 1.



140 **Figure 3.** Cumulative rainfall during 15 – 18 June 2013 in the upstream region of the UGB obtained from the Tropical Rainfall Measuring Mission Multi-Satellite Precipitation Analysis (TMPA) 3B42V7 product at 0.25° resolution.

Table 1. Comparison of TMPA data with station data

Station	Mean Absolute Error (mm)	Root Mean Square Error (mm)	Bias (%)
Uttarakashi	64	97	-40
Tehri	63	83	-44
Mussoorie	75	94	-6
Dehradun	126	191	-70
Joshimath	51	55	-21
Chamoli	44	55	-27
Rudraprayag	48	53	-22
Pauri	34	44	37
Deoprayag	95	98	-56
Hardwar	83	114	-76
Roorkee	64	82	-39
Ranikhet	71	77	27
Almora	26	30	63
Mukteshwar	90	118	-60
Nainital	86	111	-67
Haldwani	115	157	-80
Pithoragarh	56	69	-6
Champawat	100	126	1



145 TMPA data is observed to behave differently for different ranges of rainfall values over the study domain. TMPA
 overestimated the rainfall at stations with cumulative rainfall less than 200 mm (e.g., Pauri and Almora). In contrast,
 rainfall at stations receiving more than 250 mm of cumulative rainfall is underestimated. Stations that received
 rainfall of 200 – 250 mm are well represented in the TMPA data (e.g., Mussorie, Pithogarth and Champawat). From
 the analysis, it could be inferred that in the TMPA data rainfall values are clustered towards the mean value. Errors
 noticed in the TMPA data could be attributed to two factors: first, large spatial coverage and coarse resolution of the
 150 TMPA data, and second, for comparison with the observed data a simple approach of selecting nearest grid point is
 implemented.

2.2 CORDEX Data

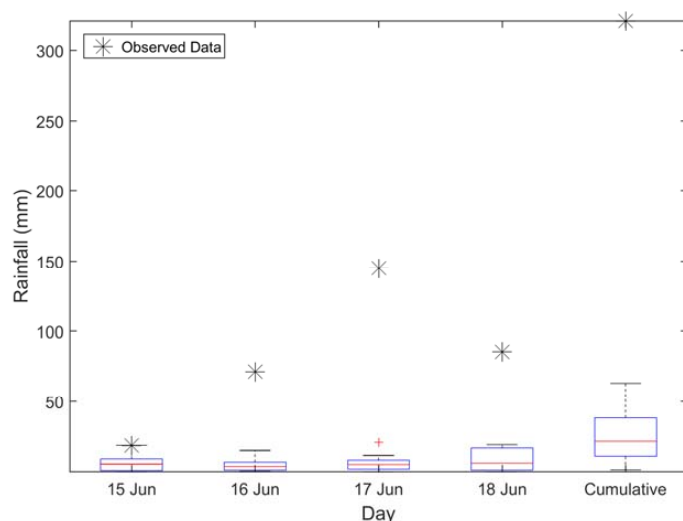
The Coordinated Regional Climate Downscaling Experiment (CORDEX; <http://www.cordex.org/>) aims at providing
 high-resolution climate projections for historic and future time periods. To achieve this, climate scenarios from the
 155 Atmosphere-Ocean coupled General Circulation Models (AOGCMs) under Coupled Model Intercomparison Project
 Phase 5 (CMIP5) are dynamically downscaled. For downscaling limited domain, relatively finer resolution Regional
 Climate Models (RCMs) are used with lateral boundary conditions from the coarse resolution AOGCMs. RCMs
 resolve the topographic details and land surface heterogeneity in order to obtain climate variables at finer spatial
 scales, in contrast to the driving AOGCMs. CORDEX provides data for historic simulations from 1971 to 2005 and
 160 future projections from 2006 to 2099/2100. For the present paper, CORDEX data corresponding to dynamically
 downscaled projections from six CMIP5 AOGCMs at 0.5° (~ 50 km) resolution (Table 2), for two Representative
 Concentration Pathways (RCPs), RCP 4.5 and RCP 8.5 are procured from Centre for Climate Change Research
 (CCCR), India (<http://cccr.tropmet.res.in/home/cordexsa.jsp>).

Table 2. List of six CMIP5 AOGCMs considered to obtained CORDEX dynamically downscaled RCM simulations

Driving AOGCMs	Institution	Downscaling RCMs
ACCESS1.0	CSIRO	Commonwealth
CNRM-CM5	Centre National de Recherches Meteorologiques	Scientific and
CCSM4	National Center for Atmospheric Research	Industrial Research
GFDL-CM3	Geophysical Fluid Dynamics Laboratory	Organization,
MPI-ESM-LR	Max Planck Institute for Meteorology (MPI-M)	(CSIRO) Australia
NorESM1-M	Norwegian Climate Centre	CCAM

165

Rainfall values from 15 to 18 June 2013 (consistent with the observed data) extracted from 12 climate scenarios (6
 models × 2 RCPs), are presented as boxplots in Figure 4. CORDEX grids falling within the geographic extent of
 Domain 2b, along with the rain gauge data are spatially averaged to obtain single rainfall value for each day.



170 **Figure 4.** Boxplot presenting the variability in daily and cumulative rainfall obtained from the CORDEX downscaled data for six models and two RCPs for 15 to 18 June 2013.

The CORDEX projections significantly underestimate the heavy rainfall event. Further, negligible variability is observed across the models for all the days except 18 June, indicating that none of the models is able to capture the realistic magnitude of the event. A few models (NorESM1-M with RCP 4.5 and ACCESS1.0 with RCP 8.5) simulated rainfall close to the observed value of 18 mm for 15 June. Cumulative rainfall across all the models has relatively higher variability, primarily due to the variability in heavy rainfall on 18 June. From the analysis, it can be concluded that the CORDEX data is capable of estimating the qualitative features of the rainfall and has significant under-prediction, indicating that care must be exercised while using the data for applications involving heavy rainfall events, such as flood modelling.

175
180

2.3 Model Configuration and Experimental Setup

The simulation experiments in this paper are conducted using the Advanced Research Weather Research and Forecasting (ARW-WRF, or simply WRF) model, version 3.8. WRF is a widely used, NWP non-hydrostatic, mesoscale model, available with several advanced physics and numerical schemes, designed for better prediction of atmospheric processes. The model description and updates can be found from (Skamarock et al., 2005) and the WRF user webpage (<http://www2.mmm.ucar.edu/wrf/users/>).

185

The WRF model utilizes large-scale atmospheric forcing as input for initialization and lateral boundary condition. These large-scale conditions are regridded by the model domain considering the grid spacing, and local topographical as well as other terrain conditions. As is common for most WRF studies over the Indian region, National Centers for Environmental Prediction (NCEP) global FiNaL (FNL) analysis dataset, based on Global Data Assimilation System (GDAS) with Global Forecast System (GFS) is considered. The FNL data is available at a coarse resolution of $1^\circ \times 1^\circ$, at every six hours' interval – 00, 06, 12 and 18 UTC (Coordinated Universal Time) and is used to provide initial and boundary conditions to the model. The WRF model is initialized using the FNL dataset

190



from 14 June 2013:00 UTC through 19 June 2013:00 UTC, for 121 hours of forecast that was output at 1-hour
195 interval. The lateral boundary conditions in the WRF model are updated at 6-h intervals. Considering the short
duration of the run, the model was forced with fixed Sea Surface Temperature (SST) throughout the integration, and
no regional data assimilation is carried out. The land surface boundary conditions are taken from the Moderate
Resolution Imaging Spectroradiometer (MODIS) International Geosphere–Biosphere Programme (IGBP) 21-
category landuse/cover fields that are available with a horizontal grid spacing of 10 min. Three telescopically-nested
200 domains are used in this study – the parent domain (Domain 1) is fixed between 60°E and 100°E with grid-spacing
of 27 km; the first nested domain (Domain 2a) covers 70–85°E, 22–37°N with 9 km grid spacing and is indicative of
“global to regional scale” (G2R) downscaling; and the second nested domain (Domain 2b) covers 76–81.5°E and
28.5–34°N at 3 km grid spacing (Fig. 1), for “global to convective scale” (G2C) downscaling (Trapp et al., 2007).
The parent domain provides lateral boundary conditions to the inner domains, resulting in the downscaling ratios for
205 simulations as 1:3 and 1:9. The three domains use 30 vertical pressure levels, with the top fixed at 50 hPa. Model
time steps were function of grid spacing: 135 s, 45 s and 15 s respectively for the three domains.
The model configuration used default parameterization options following (Osuri et al., 2012). For example,
shortwave radiation is based on Dudhia (Dudhia, 1989), and long wave based on Rapid Radiative Transfer Model
(RRTM; (Mlawer et al., 1997)) scheme. Other physical parameterization options such as Microphysics (MP),
210 Cumulus (CU) parameterization schemes, Planetary Boundary Layer (PBL) and Land Surface Models (LSMs) were
selected as outlined ahead. There is currently no known unique configuration that can best simulate an extremely
heavy rainfall event. Therefore, based on literature (e.g. Kumar et al., 2008; Hong and Lee, 2009; Misenis and
Zhang, 2010; Mukhopadhyay et al., 2010; Argüeso et al., 2011; Cardoso et al., 2013; Efstathiou et al., 2013), four
MP schemes, two CU schemes, two PBL schemes and two LSMs are considered representative to obtain an
215 ensemble of rainfall simulations. The two PBL schemes considered are the Yonsei University (YSU) scheme (Hong
et al., 2006) and the Mellor–Yamada–Janjic (MYJ) scheme (Janjić, 2001). YSU is a non-local scheme, wherein
fluxes are calculated at certain height in the PBL considering the profile of the entire domain. MYJ scheme, on the
other hand, is a local scheme in which fluxes are calculated at various heights within the PBL and are related to
vertical gradient in the atmospheric variables at the same height. Further details regarding the difference between the
220 YSU and the BMJ schemes can be obtained from (Misenis and Zhang, 2010; Efstathiou et al., 2013). The two CU
schemes considered are the Kain – Fritsch (KF) scheme (Kain, 2004) and the Betts-Miller-Janjic (BMJ) scheme
(Janjić, 1994, 2000). KF is a shallow convection scheme, based on entrainment and detrainment plume model with
updrafts and downdrafts of mass flux. Potential energy is removed in the convective time scale within this scheme.
Furthermore, it includes cloud, rain, snow and ice detrainment at cloud top. BMJ, on the other hand, considers
225 convection at both shallow and deep levels. However, there is no updraft and downdraft of mass flux and no cloud
detrainment. Domain 2b is configured without any CU scheme, assuming MP to explicitly solve the convection at
finer resolution (Sikder and Hossain, 2016). Four MP schemes considered are, the Purdue Lin (PLin) scheme (Lin et
al., 1983; Chen and Sun, 2002), the Eta Ferrier (Eta) scheme (NOAA, 2001), the WRF Single-Moment 6-class
(WSM6) scheme (Hong and Lim, 2006) and the Goddard scheme (Tao et al., 1989). Although both, the PLin
230 scheme and the WSM 6 scheme are based on the parameterization from Rutledge and Hobbs (1984), former has 5-



class microphysics while the latter has 6-class microphysics. Details of the PLin and the WSM6 schemes are available in Hong et al., (2009). The Eta scheme was designed primarily for computational efficiency in NWP models, wherein the total condensate and the water vapors are directly advected into the model. The Goddard scheme is a slight modification from the PLin scheme for ice-water saturation. In general, all the MP schemes are known to influence the rainfall simulations at fine grid resolution by influencing the water phase component (Li et al., 2017). In addition to the physics options mentioned above, two LSMs considered in the present work are, Simple 5-layer Soil Model (Slab; (Dudhia, 1996)) and the Noah LSM (Chen and Dudhia, 2001; Tewari et al., 2004). Slab is based on simple thermal diffusion in the soil layers that has constant soil moisture availability but a prognostic soil temperature term. The Noah LSM is a modestly detailed model, which includes explicit land surface parameterization with prognostic soil moisture and soil temperature evolution and snow cover prediction. (Skamarock et al., 2005)

Since each scheme is associated with a distinct feature, it is important to examine the effect of their interactions on the rainfall simulations. Table 3 provides the summary of the WRF physics schemes considered to simulate the extremely heavy rainfall event.

Table 3. Configuration of the WRF model considered for simulation of rainfall

Model Options	Dataset/Value
Domains	3
Grid Resolution (spacing)	27 km; 9 km; 3 km
Downscaling ratio	1:3; 1:9
Projection System	Mercator
Land Surface Boundary Condition	21-class MODIS
Initial Conditions	NCEP FNL
Short Wave Radiation Scheme	MM5 Shortwave or Dudhia
Long Wave Radiation Scheme	Rapid Radiative Transfer Model (RRTM)
PBL Schemes	1. Yonsei University (YSU) 2. Mellor–Yamada–Janjic (MYJ)
Cumulus Schemes	1. Kain-Fritsch (KF) 2. Betts-Miller-Janjic (BMJ)
Microphysics Schemes	1. Lin (Purdue) 2. Eta (Ferrier) 3. WSM 6 4. Goddard
Surface Layer Option	Monin-Obukhov Similarity Theory
Land Surface Models	1. Simple 5-layer Soil Model (Slab) 2. Noah

Ability of the WRF model configuration to simulate an extreme rainfall event is evaluated by comparing the simulated rainfall with the observations through indices such as Scale Error (*SE*) and Coefficient of Variation (*CV*) in addition to *MAE*, *RMSE* and β .

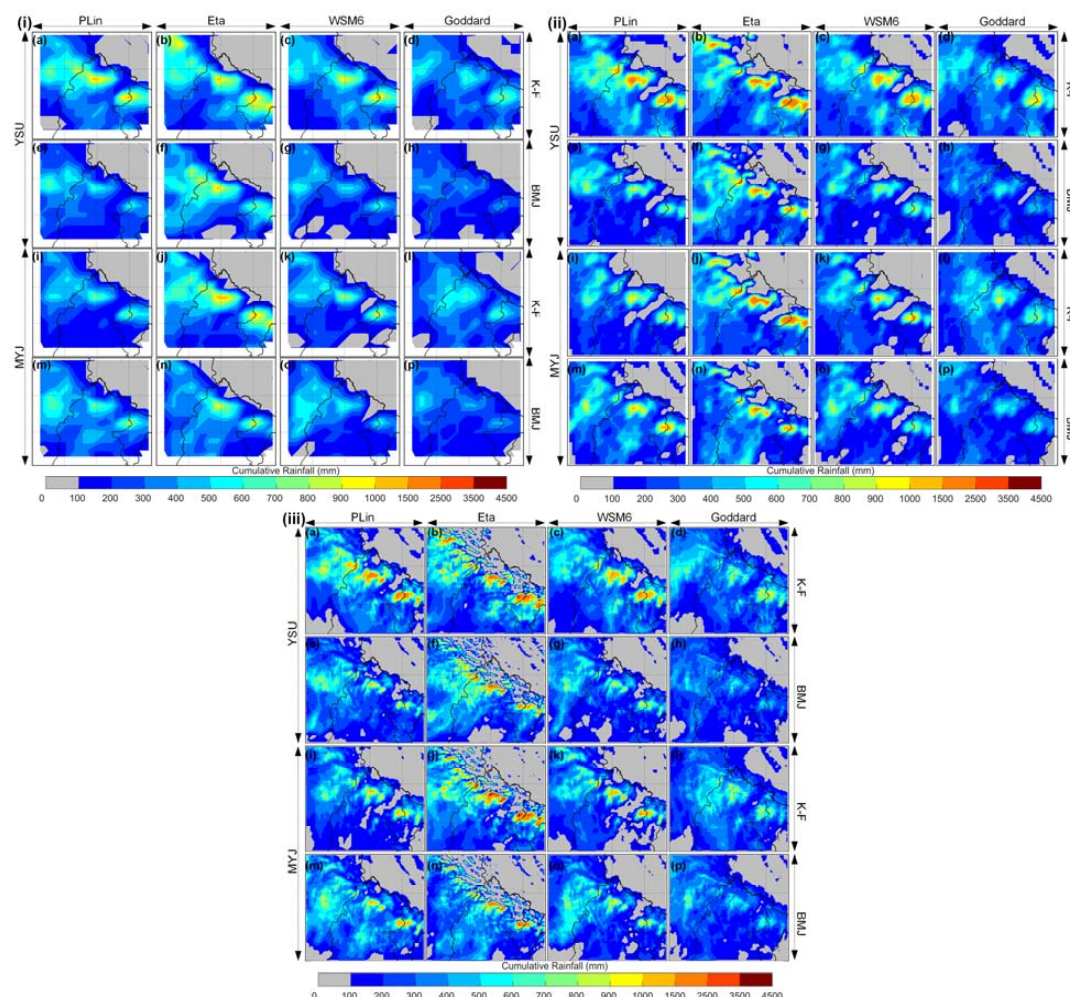


250 **3. Results and Discussion**

3.1 Sensitivity Analysis

3.1.1 Verification of WRF Simulations

Figure 5 presents cumulative rainfall for 15 – 18 June 2013 from 16 WRF simulations (4 MP, 2 CU and 2 PBL) corresponding to each of the three domains.



255 **Figure 5.** Spatial plots showing rainfall estimates obtained for (i) Domain 1; (ii) Domain 2a; and (iii) Domain 2b. Arrows in the left indicate the PBL scheme, arrows in the right represent the CU scheme and the top arrows present the MP scheme considered for the simulation runs. (a) to (p)* are the WRF configurations, for instance, Figure 5 (i) – (a) represents the WRF configuration with YSU PBL scheme, KF CU scheme and PLin MP scheme for Domain 1.
 260 *Refer to Appendix A (Table A.1) for the list of the WRF configurations.

From Figure 5 (i) to (iii), it may be seen that the spatial pattern of rainfall appears to be sensitive to the microphysics, i.e., Plin, Eta and WSM6 MP schemes, while the amount of rainfall is more dependent on the PBL and CU scheme options. There is considerable difference in the rainfall amount simulated with the Goddard MP



scheme option as compared to other MP schemes. Further, most of the model runs are able to reproduce the spatial gradient in the rainfall amount, which is perhaps primarily due to the topographical variation in the region. For locales below 1000 m, observations show distinctly lower rainfall as compared to the high elevation regions (> 1000 m). Further, distinct clusters corresponding to heavy rainfall event are observed in the northeast and northwest areas of the study region. These clusters are found to be consistent with the TMPA data; however, due to lack of surface rain gauge observations, amount of rainfall in these regions could not be verified at this stage. Incidentally, the observed heavy rainfall event in southeast part of the region is seen in a few WRF configurations, such as configuration (b) and (c). In general, WRF simulated rainfall fields show a similar spatial pattern as that of TMPA rainfall product. However, the magnitude of WRF rainfall is significantly high as compared to TMPA and is attributed to the negative bias in TMPA for heavy rains. Figure 6 summarizes the comparison of WRF rainfall with rain gauge observations for the three domains.

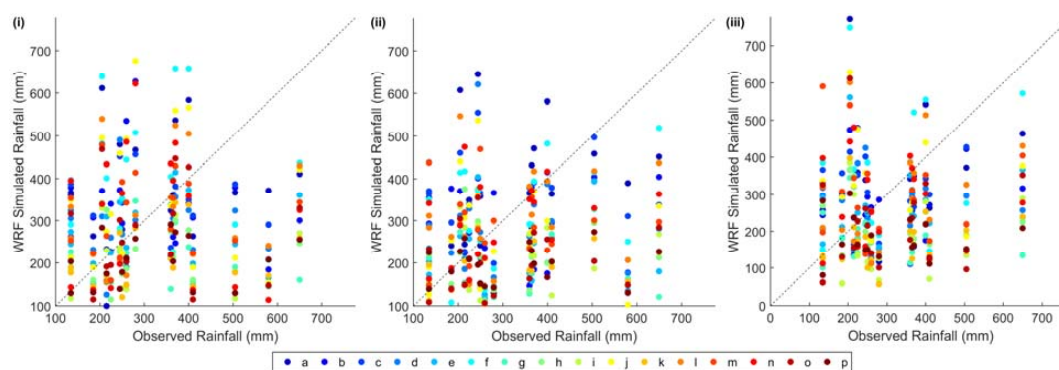


Figure 6. Scatter plots between the rainfall data from the rain gauges and the WRF simulations for (i) Domain 1; (ii) Domain 2a; and (iii) Domain 2b for (a) to (p)* WRF configurations.

*Refer to Appendix A (Table A.1) for the list of the WRF configurations.

Figure 6 indicates that Domain 1 captures rainfall within the range of 150 to 400 mm for most of the WRF configurations. For Domain 2a and Domain 2b, increase in the predicted rainfall amount is noted, particularly; for small rainfall thresholds. Further, the WRF runs still under predict extremely heavy rainfall and each of the configuration considered (across all the three domains) underestimated the rainfall amount more than 400 mm. However, the underestimation of rainfall is less in Domain 2b (G2C scale) compared to others, indicating the necessity of finer grid spacing as the first-order requirement for simulating the magnitudes of the extremely heavy rainfall events. The bias in the WRF simulations is typically due to number of interactive factors: (i) scale feedback between mesoscale convection and large-scale processes within the model (Bohra et al., 2006); (ii) lack of local observations that can add mesoscale features (Osuri et al., 2012; Osuri et al., 2015); and (iii) lack of proper land surface processes (Niyogi et al., 2006; Chang et al., 2009; Osuri et al., 2017a). To assess performance of the WRF simulations, quantitative scores (*MAE* and *RMSE*) with respect to the observed data are computed for cumulative rainfall over the 4 days' period. Results pertaining to these are presented in Figure 7.

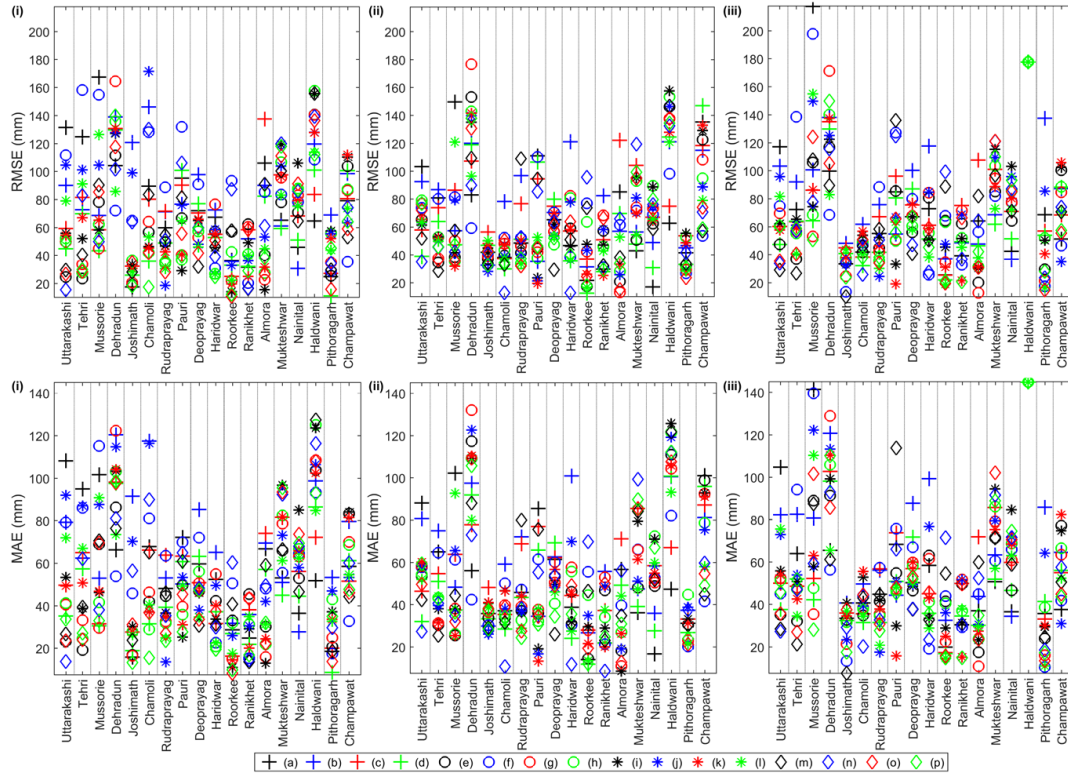


Figure 7. Root mean square error (top panel) and mean absolute error (bottom panel) computed temporally for (i) Domain 1; (ii) Domain 2a; and (iii) Domain 2b for (a) to (p)* WRF configurations.
 *Refer to Appendix A (Table A.1) for the list of the WRF configurations.

295 Figure 7 indicates that there is more error at the stations Dehradun and Haldwani, which received higher rainfall. The highest rainfall obtained in different WRF configurations for these stations was less than 500 mm and this underestimation is highlighted in the error statistics. The model results show higher error and variability in the simulations for the northern part of the domain as compared to southern. This is likely due to the complex terrain in the northern part of the domain.

300 To identify the ‘best’ and the ‘worst’ performing configurations, temporal errors across all the stations are summed up and reviewed (Appendix B, Table B.1). From this, the configuration (b) that is, YSU PBL, KF CU and Eta MP, produces maximum error, whereas configuration (p) with MYJ PBL, BMJ CU and Goddard MP, gives minimum error. This was also the ‘best’ performing configuration across all the locations for the three domains. In addition to this, spatial analysis is also conducted, wherein MAE across the 4 days’ is computed and averaged across the station

305 locations. Corresponding results are presented in Appendix B (Fig. B.1). These results are consistent to the temporal analysis and again configurations (b) and (p) give maximum and minimum error respectively. Therefore, through this analysis, it can be inferred that the WRF model with MYJ PBL, BMJ CU and Goddard MP schemes is the ‘best’ in simulating the spatial and temporal variability of the extremely heavy rainfall over the upstream region of the UGB. Why this combination emerged as the best performing is an intriguing but difficult question to address, and
 310 needs to be studied through more cases and observational analysis as it becomes available. Note that the rainfall



prediction is the combination of many nonlinear, interactive factors including behavior of each configuration and cannot be realistically studied with the sparse rainfall data and absence of vertical sounding observations. Some possible factors that could contribute would be that local boundary formulation in MYJ may be more appropriately capturing the vertical environment in the complex terrain as compared to the nonlocal YSU scheme which seeks to simulate vertical mixing and boundary layer evolution using averaged and grid representative fields (Alapaty et al., 1997). As regards to the BMJ CU emerging in the top configuration, there are a number of studies for the ISMR where it has emerged as performing “overall best” (Ratnam and Kumar, 2005; Vaidya, 2006; Rao et al., 2007; Kumar et al., 2010; Mukhopadhyay et al., 2010; Srinivas et al., 2013). As for the MP scheme, there are limited studies in comparison to those that have studied the CU configuration for the ISMR. Further, the MP scheme performance has been evaluated for tropical cyclone cases because of the warm versus cold pool processes that are critical in the simulation of the cyclone intensity. Of those available in literature, studies such as Sing and Mandal (2014) found that the Goddard scheme has a “slightly better” performance than other schemes. This conclusion is also supported by studies such as Choudhury and Das (2017) and has been used in hailstorm studies such as Chevuturi et al., (2014). Note that in citing these studies there is no claim being made about proving or even explain why the configuration that has emerged as the ‘best’ is indeed such. What these studies do provide is a reasonable basis to support the notion that the ‘best’ configuration that has emerged is realistic and plausible to be considered as such.

The impact of downscaling ratio on the rainfall simulations is addressed next. On comparing the simulations from G2R and G2C domains with the rain gauge data, it is noted that the former gives less error for most of the locations (Appendix C). G2C scale has large resolution (grid spacing) gap from outer to inner domain in comparison to G2R, which could result in less accurate initial and lateral boundary conditions, and consequently, more simulation errors in G2C. Another possibility is that the metric being used, which is the rainfall observation from in-situ data, itself is more conservative with regards to the grid in which rainfall occurs in the coarser domain and may slightly favor the G2R. However, on reviewing the overall structure of rainfall fields and the amounts across the domain, results suggest that the G2R scale with moderate downscaling ratio may be better suited for simulation of the extreme rainfall event as in the present case study. The results are found to be consistent with other studies, such as by Liu et al., (2012), wherein moderate ratio of 1:3 is found to perform best. However, it is to be noted that errors corresponding to the grid point nearest to the rain gauge are considered here for comparison. Result may vary upon selection of another grid point.

3.1.2 Impact of Different Parameterization Schemes

Although configuration (p), with MYJ PBL, BMJ CU and Goddard MP, appears to be the ‘best’ physics configuration for the study region, significant variability exists among the simulations pertaining to different configurations of the WRF model. This variability causes significant uncertainty across different runs, which is quantified through computation of *SE* and *CV* (Fig. 8 and 9). Deviation in model simulations with respect to observed data provides the *SE*, however, *CV* gives variation within different model simulations.

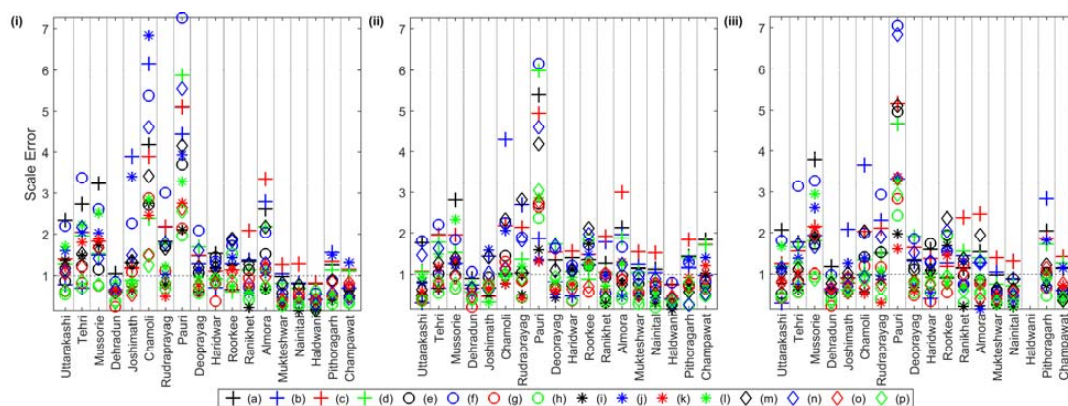


Figure 8. Scale error (*SE*) in (a) to (p)* WRF configurations for 18 locations in the UGB for (i) Domain 1; (ii) Domain 2a; and (iii) Domain 2b.

350 *Refer to Appendix A (Table A.1) for the list of the WRF configurations.

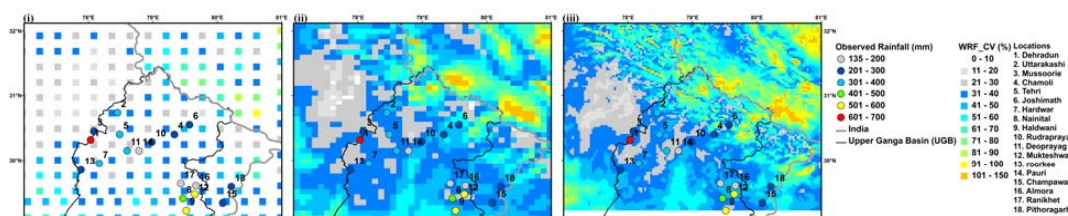


Figure 9. Coefficient of Variation (*CV*) value across different WRF configurations in the UGB for (i) Domain 1; (ii) Domain 2a; and (iii) Domain 2b.

355 Most of the model configurations have *SE* value clustered around 1 (Fig. 8), indicating that the variability in simulated rainfall is similar to the observed rainfall. However, variability in northeastern part of the domain is observed to be high compared to others. Same is reflected in the *CV* plot (Fig. 9), wherein grid points around the Chamoli station (on the northeastern side) have *CV* between 41-51 %, whereas stations closer to Uttarakashi and Tehri have values ranging between 11 – 30 %. Further, grid points closer to Dehradun have low *CV* value, which could be due to the models consistently underestimating the rainfall in this subdomain. Southern part of the region, which received low rainfall, also exhibited high variability. In general, it can be inferred that uncertainty in rainfall is more in the northeastern part compared to northwest. The regions that received very high or very low rainfall during this period also displayed higher uncertainty. Uncertainty in rainfall simulations varies between the domains, with Domain 2b having maximum uncertainty. This could be attributed to high variability in the simulated values at higher spatial resolution.

360 Since consideration of different parameterization schemes is the reason for variability in rainfall simulations, it is of interest to understand how former influences the model output. For this, the average cumulative rainfall over the region, across different configurations is considered. The differences between various configurations is evaluated to assess the influence of PBL, CU and MP parameterization schemes on the rainfall simulations. Results for the same are presented in Figure 10.

370

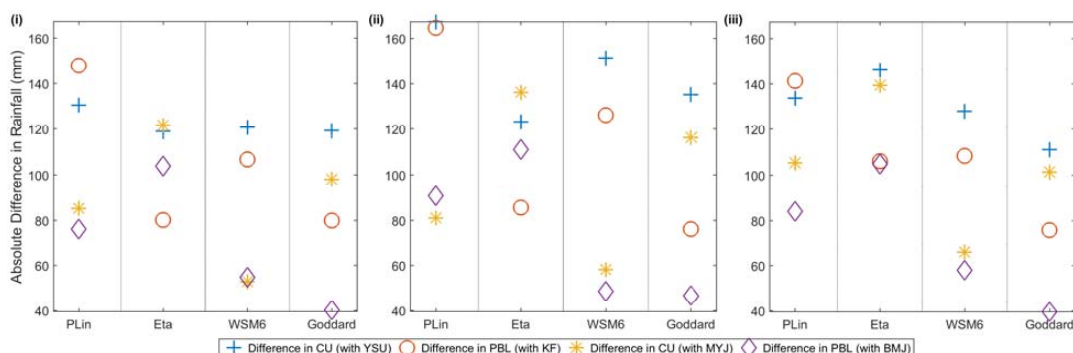


Figure 10. Difference in simulated rainfall due to PBL, CU and MP parameterization schemes corresponding to (i) Domain 1; (ii) Domain 2a; and (iii) Domain 2b over the UGB region.

It is noticed that, in general, the WRF configurations with KF convective scheme produce rainfall of higher magnitudes. This result is consistent with previously conducted studies (Gallus Jr, 1999; Fonseca et al., 2015; Pieri et al., 2015). For PLin MP, it is noted that considering YSU PBL along with KF CU scheme has a synergistic effect, leading to maximum amount of rainfall over the region. This additive effect could be attributed to the YSU being a non-local scheme making it suitable to convective, unstable PBL conditions (Bright and Mullen, 2002). Upon changing the PBL scheme (from YSU to MYJ), and maintaining the convective scheme as KF, notable difference in the fields is simulated (as shown by red circles in Fig. 10). This difference obtained for changing the PBL (with PLin MP and KF CU), is found to be either equivalent to or more compared to the case when only CU is changed (from KF to BMJ) under either YSU (shown by blue plus sign in Fig. 10) or MYJ PBL (shown by yellow star in Fig. 10) conditions. BMJ CU, irrespective of the PBL scheme, results in less simulated rainfall across the region. Therefore, it can be inferred that with PLin MP, CU plays a dominant role in determining the amount of rainfall over the region. For WSM6 MP, within YSU PBL scheme, changing the CU (from KF to BMJ) parameterization produces significant variability (displayed by blue plus sign) in rainfall than changing the PBL scheme itself (from YSU to MYJ PBL with KF CU). However, with MYJ PBL, the effect of changing CU scheme is insignificant (yellow star in Fig. 10). Furthermore, with BMJ the difference in rainfall produced due to changing the PBL is minimal. With Eta and Goddard MP, CU schemes have significant influence on rainfall irrespective of the PBL condition. It can be concluded from this section that, for Eta and Goddard MPs, the choice of PBL and CU schemes dominates the rainfall simulation. The relationship between PBL and CU for PLin and WSM6 MPs is interlinked and the choice of CU appears to have dominant impact on the simulation of rainfall over the region.

3.1.3 Impact of Land Surface Boundary Condition

The main differences in the two LSMs – Slab and Noah, considered here are related to (i) the soil depths along with the inclusion of land surface processes and (ii) the temporal evolution of soil moisture. Slab is a relatively simple LSM with 5 soil layers (at 1, 2, 4, 8 and 16 cm depths) and uses a thermal diffusion equation to compute surface fluxes based on a surface temperature and drag coefficient formulations. Noah LSM is modestly detailed (compared to Slab) LSM with 4 soil layers (at 10, 30, 60 and 100 cm depths) and explicit representation of land surface parameters, which includes the effect of soil moisture changes, snow cover, evapotranspiration and hydrologic



400 processes such as runoff and drainage (to sub surface layers). Further, in the Noah LSM soil moisture and
 temperature is prognostically computed for each of the 4 soil layers, whereas in the Slab LSM only soil temperature
 is prognostic and moisture is considered as a constant value based on the land-use. To understand the influence of
 each LSM on the rainfall estimation, simulations using the Slab LSM are conducted for the ‘best’ and the ‘worst’
 performing configurations from the Noah LSM case ((p) and (b), respectively). Results comparing the two land
 405 model based runs are presented in Figure 11.

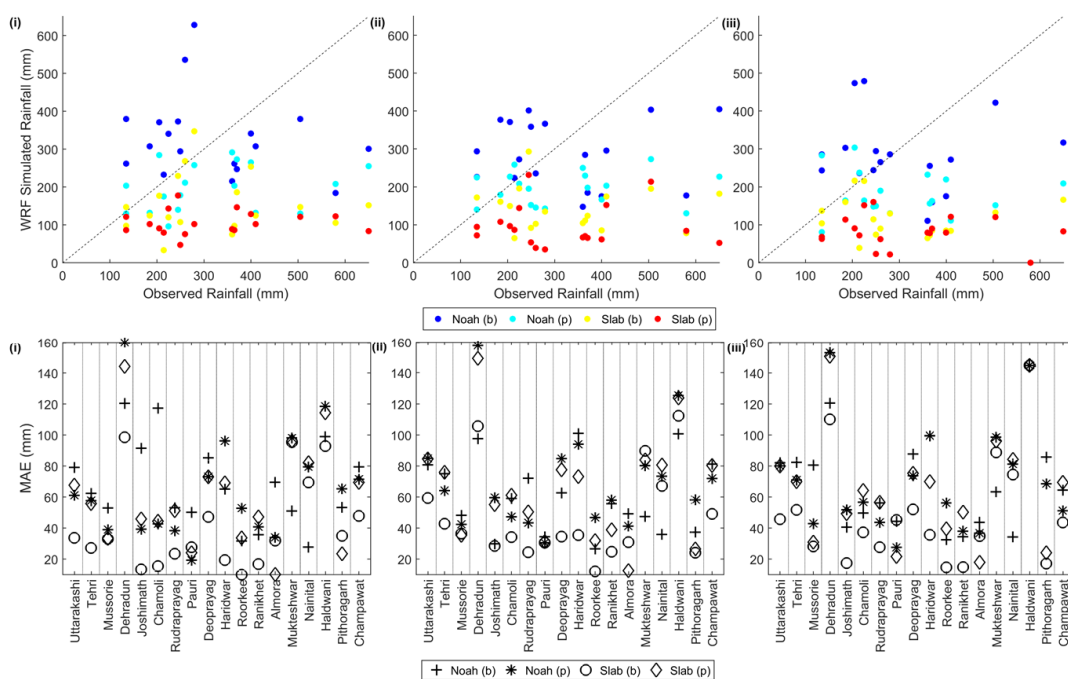


Figure 11. Scatter plot (top panel) and mean absolute error (bottom panel) for the observed rainfall data and the WRF simulations (for (b) and (p) configurations) pertaining to Noah and Slab LSMs corresponding to (i) Domain 1; (ii) Domain 2a; and (iii) Domain 2b.

410 The Slab LSM based run significantly underestimates the rainfall in comparison to the Noah LSM. For example, the
 locations which recorded rainfall greater than 400 mm have the Slab LSM based simulated values in the range of
 100 – 150 mm. As stated earlier, although Noah LSM also underestimated the rainfall for such stations, the bias with
 the Noah LSM is significantly less than the Slab LSM (-26 % with the Noah LSM, in contrast to -64 % with the Slab
 LSM for domain 2a and (p) configuration). Further, *MAE* in rainfall is also found to be higher with the Slab LSM in
 415 comparison to the Noah LSM. This is essentially due to significant underestimation of rainfall during 16 and 17 June
 2013 by the Slab LSM.

In a number studies, the differences in the surface energy fluxes simulated by the choice of different LSMs i.e. Slab
 versus Noah has been discussed (see (Niyogi et al., 2016) for a review). The main reason being that the surface
 processes affect the boundary layer feedbacks which in turn create zones of mesoscale convergence that can affect
 420 the location and intensity of convection. These convective systems then contribute to the simulated rainfall. The
 results obtained in this study emphasize this feature with differences in the rain amounts and locations through the



domain in response to the change in LSM. Better performance of using Noah model could be attributed to temporal evolution of soil moisture fields and thus, the importance of soil moisture initialization over India for extreme weather conditions is highlighted through this work (Osuri et al., 2017a).

425 3.2 Comparison between Rainfall from the WRF, CORDEX and FNL datasets

Simulated rainfall from the WRF model runs is assessed with respect to the CORDEX downscaled data and the NCEP FNL reanalysis dataset. To achieve this, it is necessary to bring all the datasets to a common spatial resolution. Therefore, WRF simulated rainfall is upscaled, through averaging of the grids, to match the resolution of NCEP FNL ($1^\circ \times 1^\circ$) and CORDEX ($0.5^\circ \times 0.5^\circ$) data. For the analysis, simulations pertaining to the ‘best,’
 430 performing configuration (p), are only considered. Bias (β) in rainfall simulations from the three datasets corresponding to 18 rain gauge locations is obtained, results for which are presented in Figure 12.

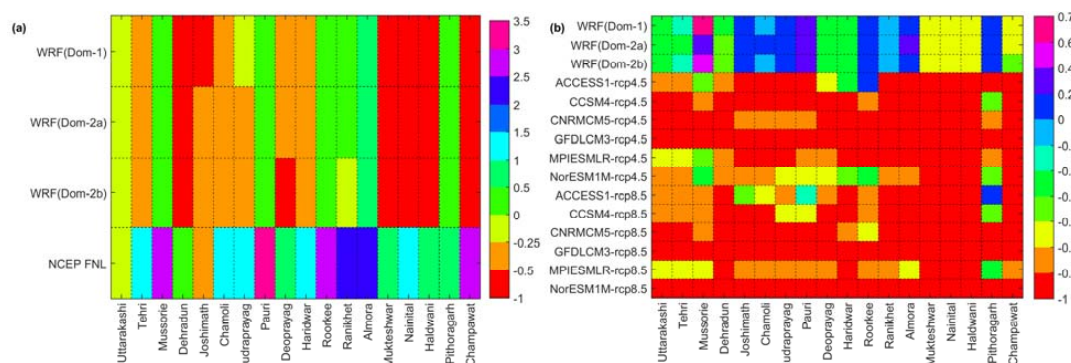


Figure 12. Bias (β) in rainfall simulations obtained from the (a) NCEP FNL and WRF (upscaled to $1^\circ \times 1^\circ$) data; and the (b) CORDEX and WRF (upscaled to $0.5^\circ \times 0.5^\circ$) data.

435 From Figure 12 (a), it can be observed that the NCEP FNL data overestimates the rainfall for most of the locations. Upon dynamic downscaling of the FNL data through the WRF model, rainfall simulations improved over the UGB region. Locations such as Mussorie, Pauri and Roorkee, which have shown β between 2.5 to 3.5 in the FNL data, reduced to 0 to 0.25 in the WRF simulations. Uttarakashi and Pithoragarh locations having small bias in the FNL data, show similar small bias in the WRF simulations. Dehradun along with three stations from south-eastern region,
 440 (Mukteshwar, Haldwani and Nainital), which recorded heavy rainfall (Section 2.1), are observed to have small bias in the FNL data, and the rainfall at these location is underestimated by the WRF model. Overall, rainfall simulations from the WRF model (for all the three domains) have less β compared to the FNL data even after upscaling to the resolution of $1^\circ \times 1^\circ$. As expected, upon upscaling, the spatial variability between the domains is reduced due to averaging across several grid points.

445 Figure 12 (b) presents comparison between the CORDEX data and the WRF simulations upscaled to the resolution of 0.5° . Rainfall is underestimated across all the locations by the CORDEX downscaled data, with most of the models having β in the range of -0.9 to -1. The WRF simulations are observed to have less β compared to the CORDEX data. Locations in the northeast along with Roorkee, Ranikhet, Almora and Pithoragarh from the southern part of the region are noticed to have negligible β in the WRF simulations. Northwestern locations (except



450 Mussorie) have shown slight underestimation within the range of -0.2 to -0.5. Only three locations, Mukteshwar, Nainital and Haldwani, which are not simulated well by the WRF model (Section 3.1.1), have shown maximum underestimation in the range of -0.6 to -0.8. It is noticed that despite upscaling, spatial variability is preserved in the WRF simulations which is not seen in the CORDEX data, wherein rainfall is consistently underestimated, within the same range, across all the locations. In addition to this, slight variability in rainfall across the three domains is
455 noticed unlike the earlier case (a), wherein the WRF simulations are compared with the NCEP FNL data. This is attributed to the fact that in this case the simulated data is upscaled to 0.5° , whereas in the previous case it was upscaled to 1° .

From the above analysis, it is evident that the WRF model can simulate extreme precipitation better than the CORDEX data and the reanalysis data. This can be attributed to increase in spatial resolution, and better
460 representation of surface and meteorological features, with respect to the lateral boundary conditions as suggested in some of the previous works such as by Argüeso et al., (2011); Mishra et al., (2014); Giorgi and Gutowski Jr (2015); Singh et al., (2017).

4. Summary and Conclusions

The main aim of this study is to provide a general guideline for setting up the WRF model configuration to simulate
465 heavy rainfall events. For the analysis, an extremely heavy rainfall event, which occurred from 15 to 18 June 2013, over the Ganges basin, in the foothills of Himalayas in the Uttarakhand State of northern India is considered. Ensemble experiments are conducted with the WRF model with different grid spacing, four microphysics schemes, two cumulus parameterization schemes, two planetary boundary layer schemes and two land surface model conditions. The rainfall simulations are evaluated against the observed rain gauge data and the TMPA precipitation
470 data. The WRF configuration with Goddard microphysics, Mellor–Yamada–Janjic planetary boundary layer condition and Betts–Miller–Janjic’ cumulus parameterization scheme is found to perform ‘best’ in simulating this extremely heavy rain event. Although complex interactions are observed between different physics options, microphysics schemes are noticed to influence the spatial pattern of the rainfall, while the choice of cumulus scheme is found to modulate the magnitude of the simulated rainfall. Upon analyzing the impact of downscaling ratios on
475 rainfall simulations, it is concluded that downscaling from global to regional scale with moderate downscaling ratio may give least model errors and thus, be considered as suitable for reproducing the extreme rainfall event. In addition to this, effect of land surface models (LSMs) on rainfall simulations is also assessed in this paper. The Slab LSM significantly underestimates the rainfall values, and incorporating Noah helped improve the performance.

In addition to the sensitivity experiments, the WRF simulated rainfall is also compared with the CORDEX
480 downscaled data and the NCEP FNL reanalysis data. The NCEP FNL data is found to overestimate the rainfall whereas, the CORDEX downscaled data significantly underestimated this event, indicating that care must be taken while employing global datasets for regional analysis. The WRF simulated rainfall, on the other hand, has least bias. Through this, it can be established that the rainfall values obtained from the high-resolution mesoscale model can be effectively used in hydrologic models for realistic streamflow estimates.



485 The analyses presented in this paper are subjected to a few limitations: first, results are limited to the physics
parameterization schemes considered in this paper, and may vary upon inclusion of other schemes; second, the best
configuration obtained needs to be evaluated for reproducing another extremely heavy rainfall event; third, only two
sets of downscaling ratios, i.e., 1:9 and 1:3 are tested in the current work. The sensitivity of simulations pertaining to
other downscaling ratios should be tested in future; and fourth, only G2R and G2C sensitivity is assessed in this
490 work.

Acknowledgment

The work is part of study supported by the US National Science Foundation and the Government of India/MOES
National Monsoon Mission at Purdue University. Second author gratefully acknowledges the financial support of
ESSO, Ministry of Earth Sciences, Govt of India and SERB, Department of Science and Technology, Govt. of India.
495 Authors thank the climate modelling groups and the climate data portal hosted at the Centre for Climate Change
Research (CCCR), Indian Institute of Tropical Meteorology (IITM) for providing the CORDEX South Asia data.



Appendices

Appendix A

500 **Table A.1.** List of different WRF configuration

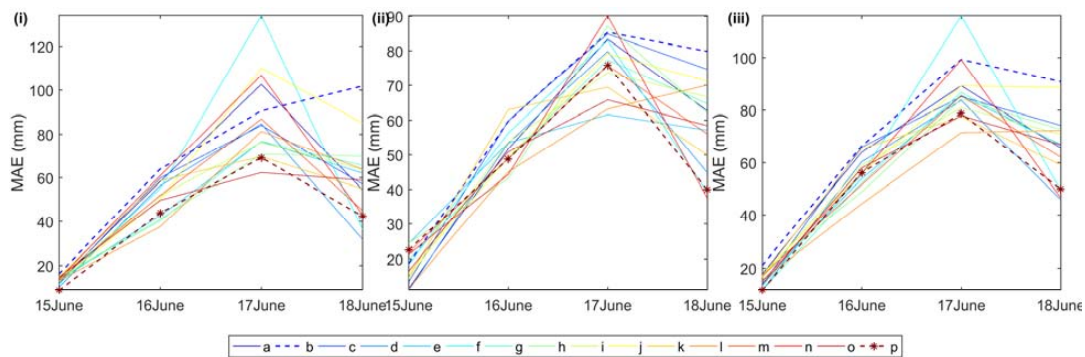
WRF Configuration	Microphysics Scheme (MP)	Cumulus Scheme (CU)	Planetary Boundary Layer Scheme (PBL)
a	PLin	KF	YSU
b	Eta	KF	YSU
c	WSM6	KF	YSU
d	Goddard	KF	YSU
e	PLin	BMJ	YSU
f	Eta	BMJ	YSU
g	WSM6	BMJ	YSU
h	Goddard	BMJ	YSU
i	PLin	KF	MYJ
j	Eta	KF	MYJ
k	WSM6	KF	MYJ
l	Goddard	KF	MYJ
m	PLin	BMJ	MYJ
n	Eta	BMJ	MYJ
o	WSM6	BMJ	MYJ
p	Goddard	BMJ	MYJ



Appendix B

Table B.1. Mean Absolute Error (MAE) values corresponding to different WRF configuration for the three domains

WRF Configuration	Domain 1		Domain 2a		Domain 2b	
	Temporal	Spatial	Temporal	Spatial	Temporal	Spatial
a	1028	228	943	210	1066	237
b	1227	273	1097	244	1249	278
c	960	213	1048	233	1077	239
d	825	183	852	189	908	202
e	877	195	885	197	995	221
f	1068	237	886	197	1055	234
g	887	197	950	211	979	218
h	885	197	976	217	1010	225
i	932	207	939	209	1024	228
j	1161	258	970	215	1131	251
k	894	199	888	197	987	219
l	883	196	855	190	918	204
m	890	198	913	203	974	217
n	1012	225	870	193	976	217
o	837	186	863	192	976	217
p	740	164	843	187	886	197



505

Figure B.1. Mean absolute errors in space corresponding to different WRF configurations for (i) Domain 1; (iii) Domain 2a; and (ii) Domain 2b. Blue dotted lines present the 'worst' performing configuration, i.e., configuration (b) and red dotted lines show the 'best' performing configuration, i.e., configuration (p).



510 Appendix C

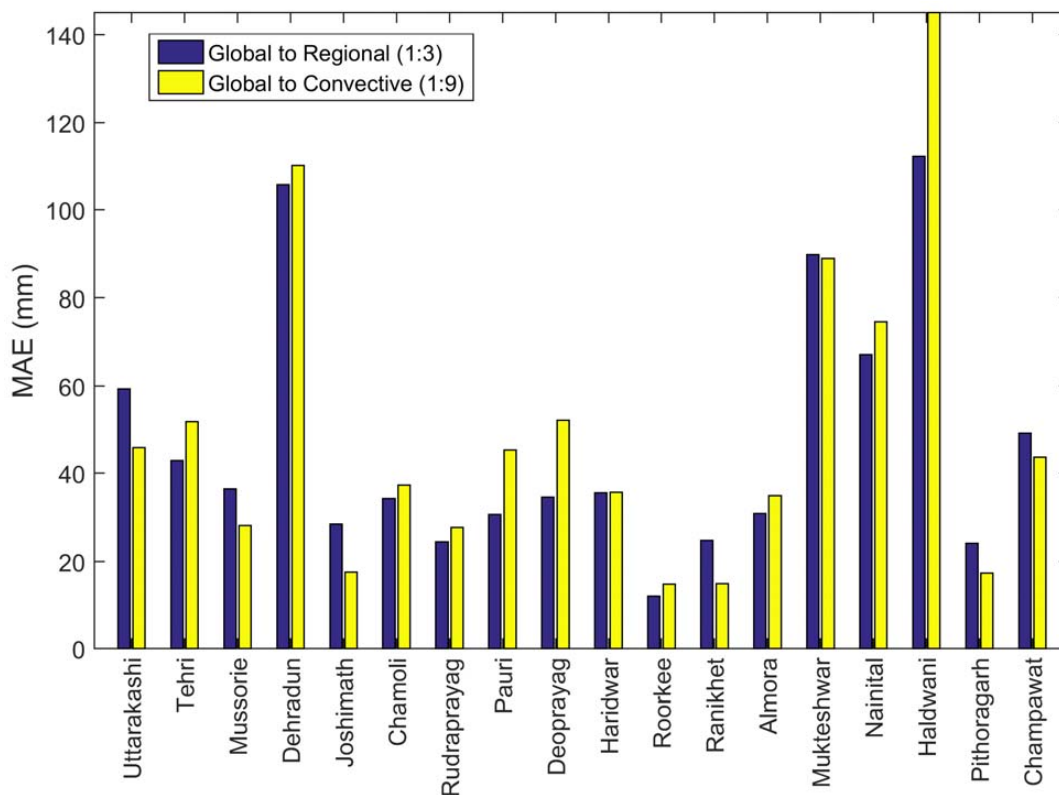


Figure C.1. Bar plot representing the mean absolute errors in simulating rainfall across the 18 rain gauge locations at Global to Regional (G2R) scale (1:3) and Global to Convection-permitting (G2C) scale (1:9).

515 **References**

- Alapaty, K., Pleim, J. E., Raman, S., Niyogi, D. S., and Byun, D. W.: Simulation of atmospheric boundary layer processes using local-and nonlocal-closure schemes, *J. Appl. Meteorol.*, 36, 214-233, 1997.
- Argüeso, D., Hidalgo-Muñoz, J. M., Gámiz-Fortis, S. R., Esteban-Parra, M. J., Dudhia, J., and Castro-Díez, Y.: Evaluation of WRF parameterizations for climate studies over Southern Spain using a multistep regionalization, *J. Clim.*, 24, 5633-5651, 2011.
- 520 Benson Jr, C. L., and Rao, G. V.: Convective bands as structural components of an Arabian Sea convective cloud cluster, *Mon. Weather Rev.*, 115, 3013-3023, 1987.
- Bohra, A., Basu, S., Rajagopal, E., Iyengar, G., Gupta, M. D., Ashrit, R., and Athiyaman, B.: Heavy rainfall episode over Mumbai on 26 July 2005: Assessment of NWP guidance, *Curr. Sci.*, 1188-1194, 2006.
- 525 Bright, D. R., and Mullen, S. L.: The sensitivity of the numerical simulation of the southwest monsoon boundary layer to the choice of PBL turbulence parameterization in MM5, *Weather and Forecasting*, 17, 99-114, 2002.
- Cardoso, R., Soares, P., Miranda, P., and Belo-Pereira, M.: WRF high resolution simulation of Iberian mean and extreme precipitation climate, *Int. J. Climatol.*, 33, 2591-2608, 2013.
- Chang, H.-I., Kumar, A., Niyogi, D., Mohanty, U., Chen, F., and Dudhia, J.: The role of land surface processes on the mesoscale simulation of the July 26, 2005 heavy rain event over Mumbai, India, *Global Planet. Change*, 67, 87-103, 2009.
- 530 Chen, F., and Dudhia, J.: Coupling an advanced land surface–hydrology model with the Penn State–NCAR MM5 modeling system. Part I: Model implementation and sensitivity, *Mon. Weather Rev.*, 129, 569-585, 2001.
- Chen, S.-H., and Sun, W.-Y.: A one-dimensional time dependent cloud model, *Journal of the Meteorological Society of Japan. Ser. II*, 80, 99-118, 2002.
- 535 Chevuturi, A., Dimri, A., and Gunturu, U.: Numerical simulation of a rare winter hailstorm event over Delhi, India on 17 January 2013, *Nat. Hazards Earth Syst. Sci.*, 14, 3331-3344, 2014.
- Chevuturi, A., Dimri, A., Das, S., Kumar, A., and Niyogi, D.: Numerical simulation of an intense precipitation event over Rudraprayag in the central Himalayas during 13–14 September 2012, *J. Earth Syst. Sci.*, 124, 1545-1561, 2015.
- 540 Choudhury, D., and Das, S.: The sensitivity to the microphysical schemes on the skill of forecasting the track and intensity of tropical cyclones using WRF-ARW model, *J. Earth Syst. Sci.*, 126, 57, 2017.
- Das, S., Ashrit, R., Iyengar, G. R., Mohandas, S., Gupta, M. D., George, J. P., Rajagopal, E., and Dutta, S. K.: Skills of different mesoscale models over Indian region during monsoon season: Forecast errors, *J. Earth Syst. Sci.*, 117, 603-620, 2008.
- 545 Deb, S., Srivastava, T., and Kishtawal, C.: The WRF model performance for the simulation of heavy precipitating events over Ahmedabad during August 2006, *J. Earth Syst. Sci.*, 117, 589-602, 2008.
- Dube, A., Ashrit, R., Ashish, A., Sharma, K., Iyengar, G., Rajagopal, E., and Basu, S.: Forecasting the heavy rainfall during Himalayan flooding—June 2013, *Weather Clim. Extr.*, 4, 22-34, 2014.
- Dudhia, J.: Numerical study of convection observed during the winter monsoon experiment using a mesoscale two-dimensional model, *J. Atmos. Sci.*, 46, 3077-3107, 1989.
- 550



- Dudhia, J.: A multi-layer soil temperature model for MM5, Preprints, The Sixth PSU/NCAR mesoscale model users' workshop, 1996, 22-24,
- Efstathiou, G., Zoumakis, N., Melas, D., Lolis, C., and Kassomenos, P.: Sensitivity of WRF to boundary layer parameterizations in simulating a heavy rainfall event using different microphysical schemes. Effect on large-scale processes, *Atmos. Res.*, 132, 125-143, 2013.
- 555 Fonseca, R., Zhang, T., and Yong, K.-T.: Improved simulation of precipitation in the tropics using a modified BMJ scheme in the WRF model, *Geoscientific Model Development*, 8, 2915-2928, 2015.
- Gallus Jr, W. A.: Eta simulations of three extreme precipitation events: Sensitivity to resolution and convective parameterization, *Weather and Forecasting*, 14, 405-426, 1999.
- 560 Giorgi, F., and Gutowski Jr, W. J.: Regional dynamical downscaling and the CORDEX initiative, *Annual Review of Environment and Resources*, 40, 2015.
- Hariprasad, K., Srinivas, C., Singh, A. B., Rao, S. V. B., Baskaran, R., and Venkatraman, B.: Numerical simulation and intercomparison of boundary layer structure with different PBL schemes in WRF using experimental observations at a tropical site, *Atmos. Res.*, 145, 27-44, 2014.
- 565 Hong, S.-Y., and Lim, J.-O. J.: The WRF single-moment 6-class microphysics scheme (WSM6), *J. Korean Meteor. Soc.*, 42, 129-151, 2006.
- Hong, S.-Y., Noh, Y., and Dudhia, J.: A new vertical diffusion package with an explicit treatment of entrainment processes, *Mon. Weather Rev.*, 134, 2318-2341, 2006.
- Hong, S.-Y., and Lee, J.-W.: Assessment of the WRF model in reproducing a flash-flood heavy rainfall event over Korea, *Atmos. Res.*, 93, 818-831, 2009.
- 570 Hong, S.-Y., Sunny Lim, K.-S., Kim, J.-H., Jade Lim, J.-O., and Dudhia, J.: Sensitivity study of cloud-resolving convective simulations with WRF using two bulk microphysical parameterizations: ice-phase microphysics versus sedimentation effects, *Journal of Applied Meteorology and Climatology*, 48, 61-76, 2009.
- Hu, X.-M., Nielsen-Gammon, J. W., and Zhang, F.: Evaluation of three planetary boundary layer schemes in the WRF model, *Journal of Applied Meteorology and Climatology*, 49, 1831-1844, 2010.
- 575 Janić, Z. I.: Nonsingular implementation of the Mellor-Yamada level 2.5 scheme in the NCEP Meso model, US Department of Commerce, National Oceanic and Atmospheric Administration, National Weather Service, National Centers for Environmental Prediction, 2001.
- Janjčić, Z. I.: The step-mountain eta coordinate model: Further developments of the convection, viscous sublayer, and turbulence closure schemes, *Mon. Weather Rev.*, 122, 927-945, 1994.
- 580 Janjić, Z. I.: Comments on "Development and evaluation of a convection scheme for use in climate models", *J. Atmos. Sci.*, 57, 3686-3686, 2000.
- Kain, J. S.: The Kain-Fritsch convective parameterization: an update, *J. Appl. Meteorol.*, 43, 170-181, 2004.
- Kneis, D., Chatterjee, C., and Singh, R.: Evaluation of TRMM rainfall estimates over a large Indian river basin (Mahanadi), *Hydrol. Earth Syst. Sci.*, 18, 2493-2502, 2014.
- 585 Kotal, S., Roy, S. S., and Roy Bhowmik, S.: Catastrophic heavy rainfall episode over Uttarakhand during 16–18 June 2013—observational aspects, *Curr. Sci.*, 107, 234-245, 2014.



- Krishnamurthy, C. K. B., Lall, U., and Kwon, H.-H.: Changing frequency and intensity of rainfall extremes over India from 1951 to 2003, *J. Clim.*, 22, 4737-4746, 2009.
- 590 Kumar, A., Dudhia, J., Rotunno, R., Niyogi, D., and Mohanty, U.: Analysis of the 26 July 2005 heavy rain event over Mumbai, India using the Weather Research and Forecasting (WRF) model, *Q. J. Roy. Meteorol. Soc.*, 134, 1897-1910, 2008.
- Kumar, M. S., Shekhar, M., Krishna, S. R., Bhutiyani, M., and Ganju, A.: Numerical simulation of cloud burst event on August 05, 2010, over Leh using WRF mesoscale model, *Nat. Hazards*, 62, 1261-1271, 2012.
- 595 Kumar, R. A., Dudhia, J., and Roy Bhownik, S.: Evaluation of Physics options of the Weather Research and Forecasting (WRF) Model to simulate high impact heavy rainfall events over Indian Monsoon region, *Geofizika*, 27, 101-125, 2010.
- Li, L., Gochis, D. J., Sobolowski, S., and Mesquita, M. D.: Evaluating the present annual water budget of a Himalayan headwater river basin using a high-resolution atmosphere-hydrology model, *J. Geophys. Res. [Atmos.]*, 600 122, 4786-4807, 2017.
- Li, X., and Pu, Z.: Sensitivity of numerical simulation of early rapid intensification of Hurricane Emily (2005) to cloud microphysical and planetary boundary layer parameterizations, *Mon. Weather Rev.*, 136, 4819-4838, 2008.
- Lin, Y.-L., Farley, R. D., and Orville, H. D.: Bulk parameterization of the snow field in a cloud model, *J. Clim. Appl. Meteorol.*, 22, 1065-1092, 1983.
- 605 Liu, J., Bray, M., and Han, D.: Sensitivity of the Weather Research and Forecasting (WRF) model to downscaling ratios and storm types in rainfall simulation, *Hydrol. Processes*, 26, 3012-3031, 2012.
- Madala, S., Satyanarayana, A., and Rao, T. N.: Performance evaluation of PBL and cumulus parameterization schemes of WRF ARW model in simulating severe thunderstorm events over Gadanki MST radar facility—case study, *Atmos. Res.*, 139, 1-17, 2014.
- 610 Misenis, C., and Zhang, Y.: An examination of sensitivity of WRF/Chem predictions to physical parameterizations, horizontal grid spacing, and nesting options, *Atmos. Res.*, 97, 315-334, 2010.
- Mishra, V., Kumar, D., Ganguly, A. R., Sanjay, J., Mujumdar, M., Krishnan, R., and Shah, R. D.: Reliability of regional and global climate models to simulate precipitation extremes over India, *J. Geophys. Res. [Atmos.]*, 119, 9301-9323, 2014.
- 615 Mlawer, E. J., Taubman, S. J., Brown, P. D., Iacono, M. J., and Clough, S. A.: Radiative transfer for inhomogeneous atmospheres: RRTM, a validated correlated-k model for the longwave, *J. Geophys. Res. [Atmos.]*, 102, 16663-16682, 1997.
- Mohanty, U., Routray, A., Osuri, K. K., and Prasad, S. K.: A study on simulation of heavy rainfall events over Indian region with ARW-3DVAR modeling system, *Pure Appl. Geophys.*, 169, 381-399, 2012.
- 620 Mukhopadhyay, P., Taraphdar, S., Goswami, B., and Krishnakumar, K.: Indian summer monsoon precipitation climatology in a high-resolution regional climate model: Impacts of convective parameterization on systematic biases, *Weather and Forecasting*, 25, 369-387, 2010.
- Niyogi, D., Holt, T., Zhong, S., Pyle, P. C., and Basara, J.: Urban and land surface effects on the 30 July 2003 mesoscale convective system event observed in the southern Great Plains, *J. Geophys. Res. [Atmos.]*, 111, 2006.



- 625 Niyogi, D., Subramanian, S., and Osuri, K. K.: The Role of Land Surface Processes on Tropical Cyclones: Introduction to Land Surface Models, in: *Advanced Numerical Modeling and Data Assimilation Techniques for Tropical Cyclone Prediction*, Springer, 221-246, 2016.
- NOAA: National Oceanic and Atmospheric Administration Changes to the NCEP Meso Eta Analysis and Forecast System: Increase in resolution, new cloud microphysics, modified precipitation assimilation, modified 3DVAR analysis, 2001.
- 630 Osuri, K., Nadimpalli, R., Mohanty, U., Chen, F., Rajeevan, M., and Niyogi, D.: Improved prediction of severe thunderstorms over the Indian Monsoon region using high-resolution soil moisture and temperature initialization, *Scientific Reports*, 7, 2017a.
- Osuri, K. K., Mohanty, U., Routray, A., Kulkarni, M. A., and Mohapatra, M.: Customization of WRF-ARW model with physical parameterization schemes for the simulation of tropical cyclones over North Indian Ocean, *Nat. Hazards*, 63, 1337-1359, 2012.
- 635 Osuri, K. K., Mohanty, U., Routray, A., and Niyogi, D.: Improved prediction of Bay of Bengal Tropical cyclones through assimilation of doppler weather radar observations, *Mon. Weather Rev.*, 143, 4533-4560, 2015.
- Osuri, K. K., Nadimpalli, R., Mohanty, U. C., and Niyogi, D.: Prediction of rapid intensification of tropical cyclone Phailin over the Bay of Bengal using the HWRF modelling system, *Q. J. Roy. Meteorol. Soc.*, 2017b.
- 640 Pieri, A. B., von Hardenberg, J., Parodi, A., and Provenzale, A.: Sensitivity of precipitation statistics to resolution, microphysics, and convective parameterization: A case study with the high-resolution WRF climate model over Europe, *J. Hydrometeorol.*, 16, 1857-1872, 2015.
- Rahman, S., Sengupta, D., and Ravichandran, M.: Variability of Indian summer monsoon rainfall in daily data from gauge and satellite, *J. Geophys. Res. [Atmos.]*, 114, 2009.
- 645 Rajeevan, M., Kesarkar, A., Thampi, S., Rao, T., Radhakrishna, B., and Rajasekhar, M.: Sensitivity of WRF cloud microphysics to simulations of a severe thunderstorm event over Southeast India, *Annales Geophysicae*, 2010, 603-619,
- Rajesh, P., Pattnaik, S., Rai, D., Osuri, K., Mohanty, U., and Tripathy, S.: Role of land state in a high resolution mesoscale model for simulating the Uttarakhand heavy rainfall event over India, *J. Earth Syst. Sci.*, 125, 475-498, 2016.
- 650 Raju, P., Potty, J., and Mohanty, U.: Sensitivity of physical parameterizations on prediction of tropical cyclone Nargis over the Bay of Bengal using WRF model, *Meteorol. Atmos. Phys.*, 113, 125, 2011.
- Rao, Y. R., Hatwar, H., Salah, A. K., and Sudhakar, Y.: An experiment using the high resolution Eta and WRF models to forecast heavy precipitation over India, *Pure Appl. Geophys.*, 164, 1593-1615, 2007.
- 655 Ratnam, J. V., and Kumar, K. K.: Sensitivity of the simulated monsoons of 1987 and 1988 to convective parameterization schemes in MM5, *J. Clim.*, 18, 2724-2743, 2005.
- Rauscher, S. A., Coppola, E., Piani, C., and Giorgi, F.: Resolution effects on regional climate model simulations of seasonal precipitation over Europe, *Clim. Dyn.*, 35, 685-711, 2010.
- 660 Ray, K., Bhan, S., and Sunitha Devi, S.: A METEOROLOGICAL ANALYSIS OF VERY HEAVY RAINFALL EVENT OVER UTTARAKHAND DURING 14-17 JUNE, 2013, *Monsoon2013*, 37, 2014.



- Routray, A., Mohanty, U., Niyogi, D., Rizvi, S., and Osuri, K. K.: Simulation of heavy rainfall events over Indian monsoon region using WRF-3DVAR data assimilation system, *Meteorol. Atmos. Phys.*, 106, 107-125, 2010.
- Routray, A., Mohanty, U., Osuri, K. K., Kar, S., and Niyogi, D.: Impact of satellite radiance data on simulations of
665 Bay of Bengal tropical cyclones using the WRF-3DVAR modeling system, *IEEE Trans. Geosci. Remote Sens.*, 54, 2285-2303, 2016.
- Rutledge, S. A., and Hobbs, P. V.: The mesoscale and microscale structure and organization of clouds and precipitation in midlatitude cyclones. XII: A diagnostic modeling study of precipitation development in narrow cold-frontal rainbands, *J. Atmos. Sci.*, 41, 2949-2972, 1984.
- 670 Shekhar, M., Pattanayak, S., Mohanty, U., Paul, S., and Kumar, M. S.: A study on the heavy rainfall event around Kedarnath area (Uttarakhand) on 16 June 2013, *J. Earth Syst. Sci.*, 124, 1531-1544, 2015.
- Sikder, S., and Hossain, F.: Assessment of the weather research and forecasting model generalized parameterization schemes for advancement of precipitation forecasting in monsoon-driven river basins, *J. Adv. Modeling Earth Sys.*, 8, 1210-1228, 2016.
- 675 Sikka, D., and Gadgil, S.: On the maximum cloud zone and the ITCZ over Indian, longitudes during the southwest monsoon, *Mon. Weather Rev.*, 108, 1840-1853, 1980.
- Sing, K. S., and Mandal, M.: Sensitivity of Mesoscale Simulation of Aila Cyclone to the Parameterization of Physical Processes Using WRF Model, in: *Monitoring and Prediction of Tropical Cyclones in the Indian Ocean and Climate Change*, Springer, 300-308, 2014.
- 680 Singh, S., Ghosh, S., Sahana, A., Vittal, H., and Karmakar, S.: Do dynamic regional models add value to the global model projections of Indian monsoon?, *Clim. Dyn.*, 48, 1375-1397, 2017.
- Skamarock, W. C., Klemp, J. B., Dudhia, J., Gill, D. O., Barker, D. M., Wang, W., and Powers, J. G.: A description of the advanced research WRF version 2, National Center For Atmospheric Research Boulder Co Mesoscale and Microscale Meteorology Div, 2005.
- 685 Srinivas, C., Hariprasad, D., Bhaskar Rao, D., Anjaneyulu, Y., Baskaran, R., and Venkatraman, B.: Simulation of the Indian summer monsoon regional climate using advanced research WRF model, *Int. J. Climatol.*, 33, 1195-1210, 2013.
- Tao, W.-K., Simpson, J., and McCumber, M.: An ice-water saturation adjustment, *Mon. Weather Rev.*, 117, 231-235, 1989.
- 690 Tewari, M., Chen, F., Wang, W., Dudhia, J., LeMone, M., Mitchell, K., Ek, M., Gayno, G., Wegiel, J., and Cuenca, R.: Implementation and verification of the unified NOAA land surface model in the WRF model, 20th conference on weather analysis and forecasting/16th conference on numerical weather prediction, 2004,
- Trapp, R. J., Halvorson, B. A., and Diffenbaugh, N. S.: Telescoping, multimodel approaches to evaluate extreme convective weather under future climates, *J. Geophys. Res. [Atmos.]*, 112, 2007.
- 695 Vaidya, S.: The performance of two convective parameterization schemes in a mesoscale model over the Indian region, *Meteorol. Atmos. Phys.*, 92, 175-190, 2006.
- Vaidya, S., and Kulkarni, J.: Simulation of heavy precipitation over Santacruz, Mumbai on 26 July 2005, using mesoscale model, *Meteorol. Atmos. Phys.*, 98, 55-66, 2007.



Zipser, E. J., Liu, C., Cecil, D. J., Nesbitt, S. W., and Yorty, D. P.: Where are the most intense thunderstorms on
700 Earth?, *Bull. Am. Meteorol. Soc.*, 87, 1057-1071, 2006.